Journal of Power Sources 225 (2013) 231–239

Contents lists available at SciVerse ScienceDirect

Journal of Power Sources

journal homepage: www.elsevier.com/locate/jpowsour

Short communication

# Investigation of Pt nanoparticles with controlled size supported on carbon for dimethyl ether electrooxidation

Fengzhan Si [a,c], Jianhui Liao [a], Liang Liang [a], Changpeng Liu [a], Xinbo Zhang [b,**], Wei Xing [a,*]

[a] State Key Laboratory of Electroanalytical Chemistry, Jilin Province Key Laboratory of Low Carbon Chemical Power, Changchun Institute of Applied Chemistry, Chinese Academy of Sciences, 5625 Renmin Street, Changchun 130022, PR China
[b] State Key Laboratory of Rare Earth Resource Utilization, Changchun Institute of Applied Chemistry, Chinese Academy of Sciences, 5625 Renmin Street, Changchun 130022, PR China
[c] Graduate University of Chinese Academy of Sciences, PR China

## HIGHLIGHTS

- Pt/C catalysts with controlled Pt particle size were synthesized without surfactant.
- Ethylene glycol was employed as both solvent and reducing agent.
- Pt particle was regulated by changing the amount of added urea.
- Electrocatalysis of DME oxidation vs. Pt particle size exists a parabolic trend.

## ARTICLE INFO

*Article history:*
Received 26 September 2012
Accepted 3 October 2012
Available online 17 October 2012

*Keywords:*
Size-controlled synthesis
Platinum catalyst
Direct dimethyl ether fuel cell
Electron transfer coefficient

## ABSTRACT

A series of Pt/C catalysts with controlled Pt particle sizes is synthesized using a surfactant-free process with ethylene glycol as the weak reducing agent. The Pt particle size can be regulated by controlling the pH of the Pt (IV) complex via the addition of different amounts of urea. The results of X-ray diffraction and transmission electron microscopy confirm that the Pt nanoparticles on the carbon exhibit good size controllability and dispersion. The electroactive surface area (ESA), the electron transfer coefficient, and the electrocatalytic activity to dimethyl ether electrooxidation are dependent on the Pt particle size, and a comparison of the electrochemical properties of the samples reveals that the relationships are parabolic. The results are important for understanding the mechanism of and designing an effective catalyst for dimethyl ether (DME) electrooxidation and providing a size-controlled synthetic method for Pt-based catalysts.



## 1. Introduction

Dimethyl ether (DME), a promising fuel for fuel cells, has been the subject of intense study in recent years due to its high energy density, ease of storage, low effect on fuel crossover, and rapid electrooxidation [1–4]. Considering their portability and lack of complicated external devices, direct dimethyl ether fuel cells (DDFCs) are particularly well suited to mobile power supply applications [5]. Most of the anode catalysts for DME electrooxidation are Pt-based [6–11], and the Pt morphology, microstructure [12,13], and doping effects [7,9,14] have been extensively investigated in an attempt to increase the catalyst activity. However, due to the recency of their development, the current understanding of DDFCs is insufficient for their practical application [2]. The catalyst performance requires further improvement, and the mechanism and contributing factors are not yet completely understood [2,4,8,10,13–17]. The Pt nanoparticle size is an especially important determinant of the adsorption power and electron transfer kinetics; thus, it has a significant influence on catalyst activity and stability [18–20].

The objective of this work is to synthesize a series of carbon-supported Pt catalysts with various Pt nanoparticle sizes to investigate the relationship between electrocatalytic performance and Pt nanoparticle size. Ethylene glycol (EG) has been selected as both the solvent and reducing agent in the preparation process because the abundant hydroxyl groups are favorable to the dispersion of carbon nanospheres and the weak reducing capacity is beneficial for adjusting the Pt growth rate. To maintain the pH throughout the reducing process, urea was used to create a buffer environment via a reversible hydrolytic process with heating. The particle size may be controlled by changing the amount of urea added without

* Corresponding author. Tel.: +86 431 85262223; fax: +86 431 85685653.
** Corresponding author. Tel./fax: 86 431 85262235.
*E-mail addresses:* xbzhang@ciac.jl.cn (X. Zhang), xingwei@ciac.jl.cn (W. Xing).

0378-7753/$ – see front matter © 2012 Elsevier B.V. All rights reserved.
http://dx.doi.org/10.1016/j.jpowsour.2012.10.021

surfactant. The size controllability has been proven by physical characterization. The effects of urea content on particle size and of particle size on the DME electrooxidation has been confirmed by electrochemical experiments.

## 2. Experimental

### 2.1. Catalyst preparation

The synthesis of the carbon-supported Pt nanoparticles was based on reference [21], which provides a method for controlling the size and dispersion of Pt nanoparticles. Based on this work, 16.3 mg of carbon nanospheres (Vulcan XC-72R), which functioned as the support, was dispersed in 100 mL of ultrapure water under ultrasonication for 30 min. Different amounts of urea were added, the mixture was subjected to an additional 30 min of ultrasonication, and then 1.730 mL of $H_2PtCl_6$ solution (14.086 $mg_{Pt}$ $mL^{-1}$) was added. After intensive stirring, the suspension was heated to 90 °C in a water bath and stirred for 1 h at constant temperature. After cooling to room temperature, the pH of the suspension was recorded. EG (100 mL) was poured into the above suspension and stirred for 3 h at room temperature. Next, the suspension was heated to 120 °C in an oil bath and stirred for 1 h. Finally, the suspension was cooled to room temperature and stirred overnight. After filtration, the product was washed with ultrapure water and dried at room temperature.

The samples with 0, 50, 100, 150, 300, and 500 mg of urea were denoted as EG-1, EG-2, EG-3, EG-4, EG-5, and EG-6, respectively. The nominal Pt content in the synthesized catalysts is 60 wt%.

### 2.2. Catalyst characterization

X-ray diffraction (XRD) measurements were performed on a Rigaku D/max 2500 diffractometer with Cu Kα radiation ($\lambda$ = 0.15405 nm) from 10° to 90° at a scanning rate of 5° per minute. The samples were ground and flattened on a slab of glass with a hole.

Transmission electron microscopy (TEM) measurements was performed were obtained using a FEI Tecnai G2 S-Twin instrument with a field emission gun operating at 200 kV, and the images were acquired digitally using a Gatan multipole CCD camera. Samples for the TEM experiments were prepared by dispersing the sample powder in ethanol, sonicating for 2 min to ensure adequate dispersion, and evaporating one drop of the suspension onto a 300 mesh Cu grid with a layer of carbon film. The bulk composition of the catalysts was evaluated by energy dispersive X-ray analysis (EDX) on a JEOL JAX-840 scanning electron microscope operating at 20 kV.

### 2.3. Electrochemical measurements

Electrochemical measurements were performed in a standard three-electrode electrolytic cell at room temperature. Pt foil and a saturated calomel electrode (SCE) were used as the counter and reference electrodes, respectively. All potentials cited in this paper were referred to SCE. All electrolyte solutions were deaerated with high-purity nitrogen for at least 20 min prior to measurement. The electrode potential was controlled by an EG&G (model 273) potentiostat/galvanostat system.

The working electrode was prepared as follows. First, 5 mg of the catalyst was dispersed in a diluted Nafion alcohol solution containing 1000 μL of ethanol and 50 μL of Nafion solution (Aldrich, 5 wt % Nafion). The resultant solution was sonicated for 30 min to obtain a uniform suspension. Next, 10 μL of the suspension was pipetted onto the flat glassy carbon electrode ($\Phi_{glassy\ carbon}$ = 4 mm, $\Phi_{electrode}$ = 6 mm). The coated electrode was then dried at room temperature for 30 min. The glassy carbon electrode was successively polished with 0.5 and 0.03 μm alumina slurries before use.

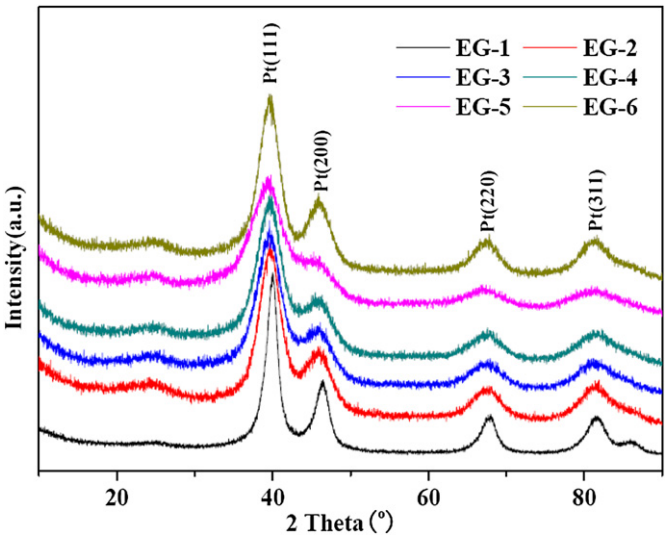


**Fig. 1.** XRD patterns of samples synthesized under different conditions.

All electrochemical measurements were performed in a 0.5 M $HClO_4$ solution with or without saturated DME. The saturated DME solution was prepared by purging DME into the 0.5 M $HClO_4$ solution for 20 min, whereas the solution without DME was deaerated by pure nitrogen for 15 min prior to measurement. The potential range for the electrooxidation of DME was from −0.2 to +1.0 V. All measurements were performed at room temperature, and the stable results were reported.

## 3. Results and discussion

During heating and stirring, urea reacts as follows:

$$CO(NH_2)_2 + 3H_2O \Leftrightarrow 2NH_4^+ + CO_2 + 2OH^- \quad (1)$$

The resultant $OH^-$ ions can form a new complex with $PtCl_6^{2-}$, which affects the rate of following reducing reaction. The Pt nanoparticle size was regulated by changing the ratio between the

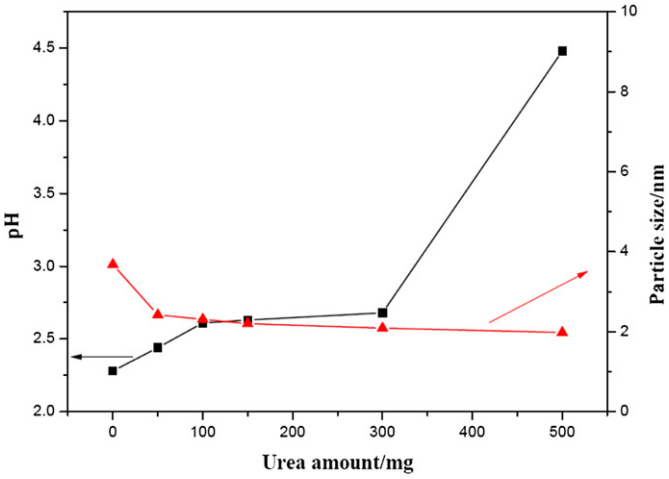


**Fig. 2.** Solution pH before reduction (left axis) and Pt nanoparticle size calculated from the XRD results (right axis) as a function of amount of added urea (horizontal axis).

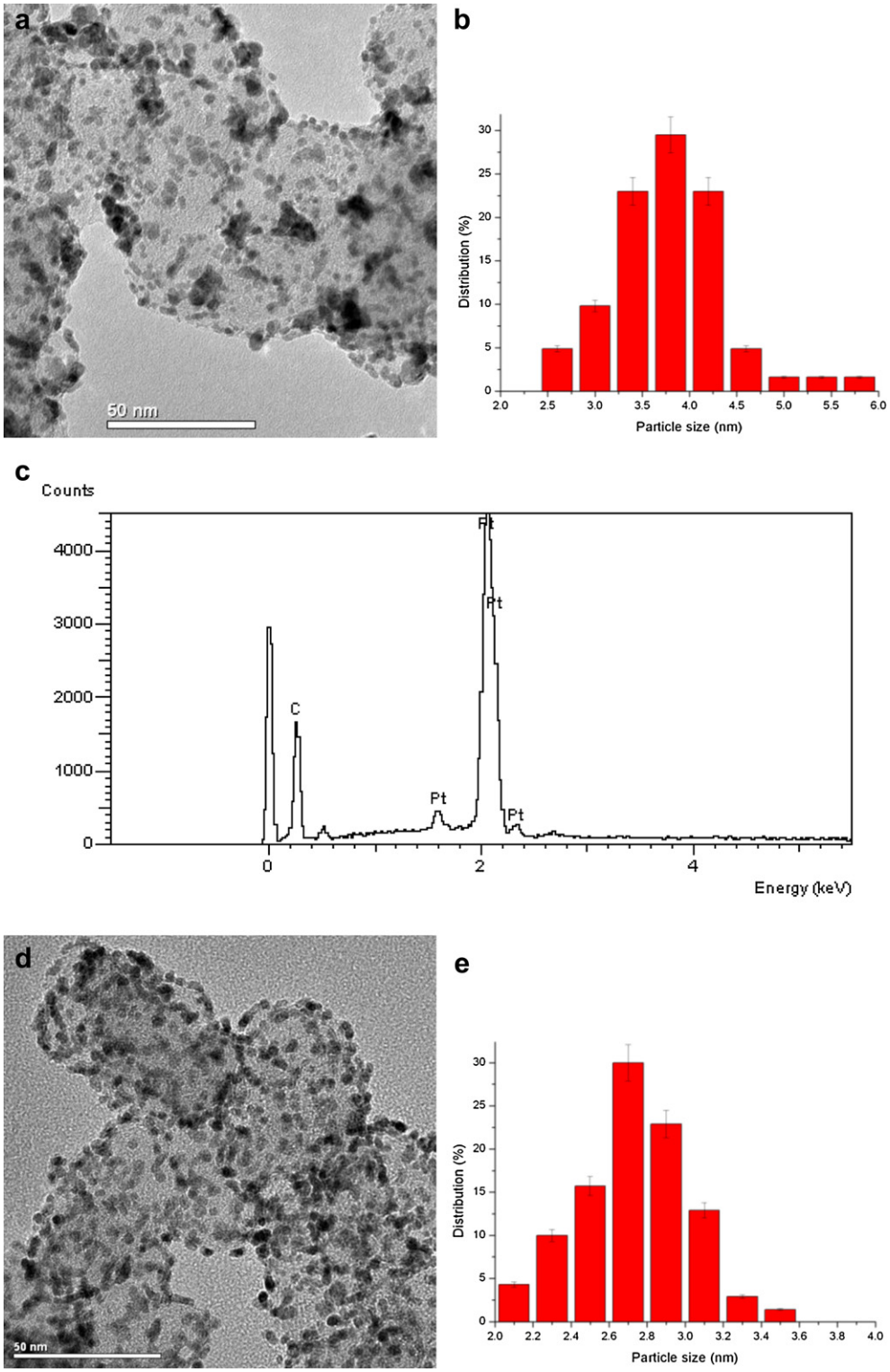


**Fig. 3.** (a), (d), (g), (j), (m), (p): TEM micrograph of EG-1, EG-2, EG-3, EG-4, EG-5, and EG-6, respectively; (b), (e), (h), (k), (n), (q): The corresponding size distribution histograms, including error bars; (c), (f), (i), (l), (o), (r): The corresponding EDX results.

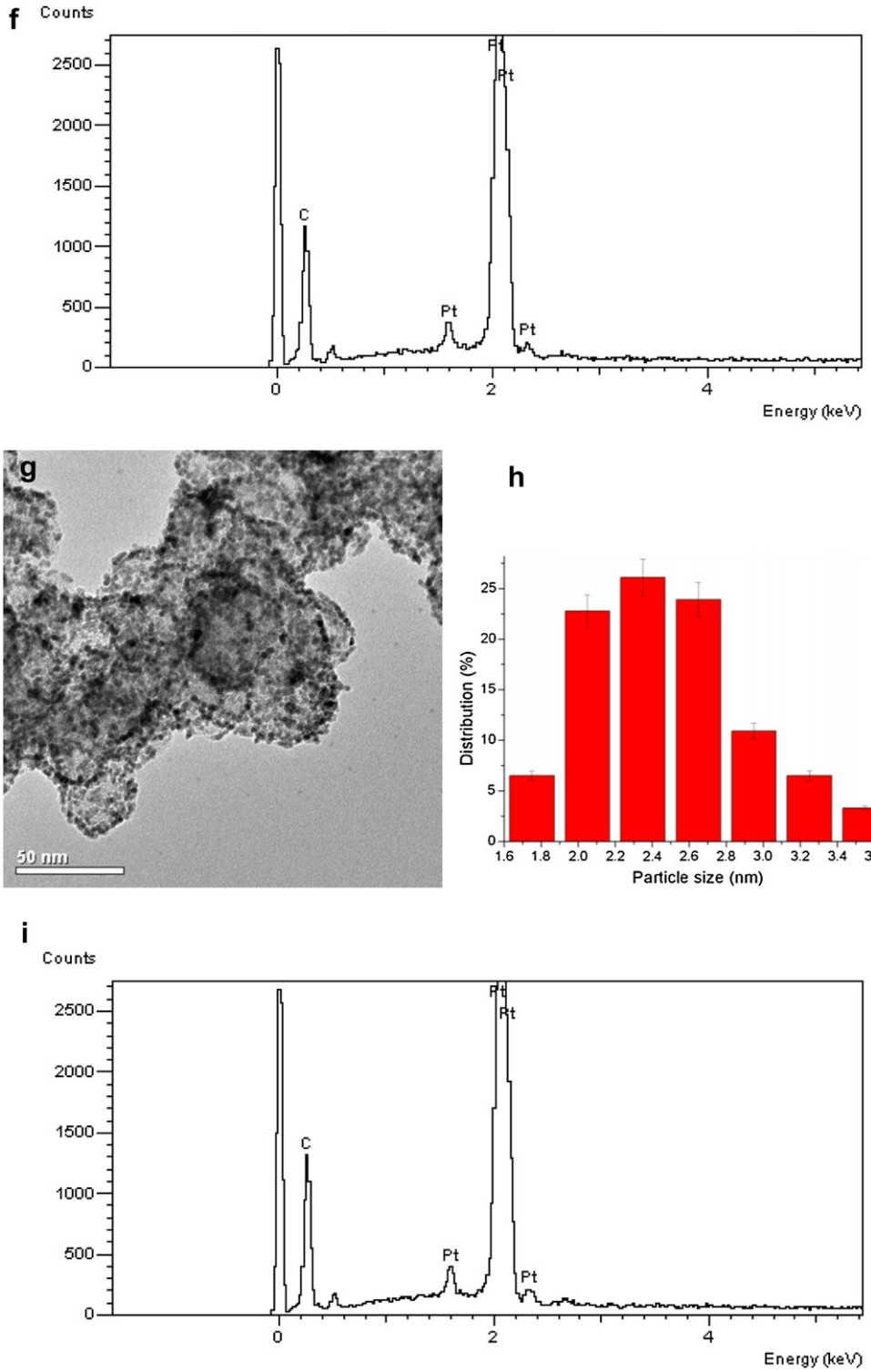


**Fig. 3.** (*continued*).

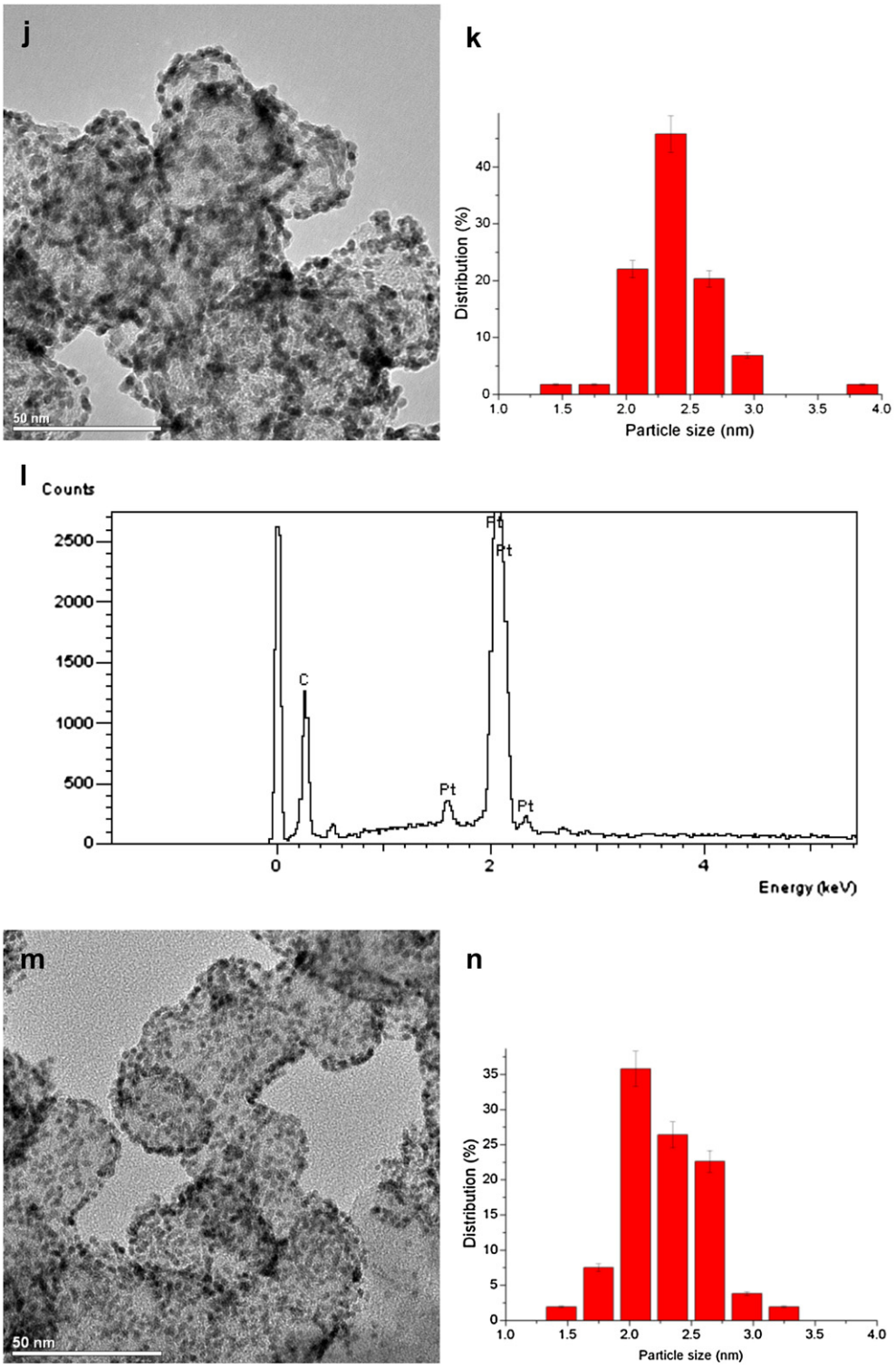


**Fig. 3.** (*continued*).

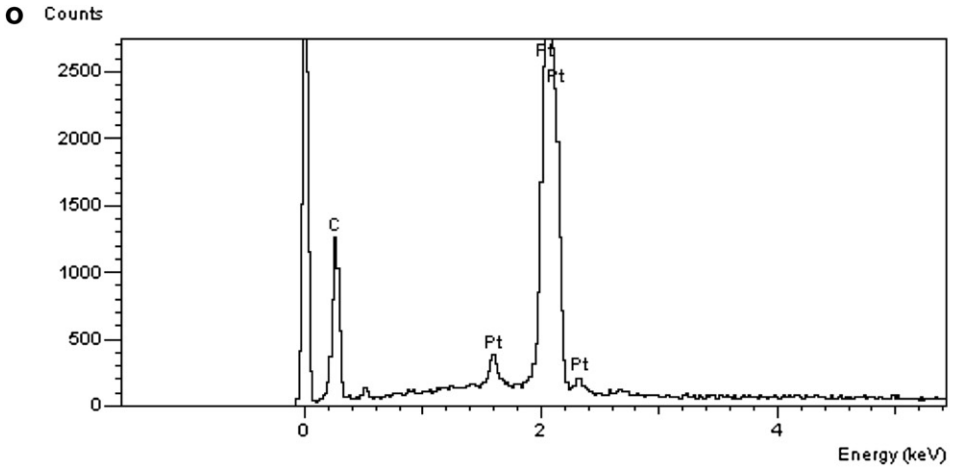


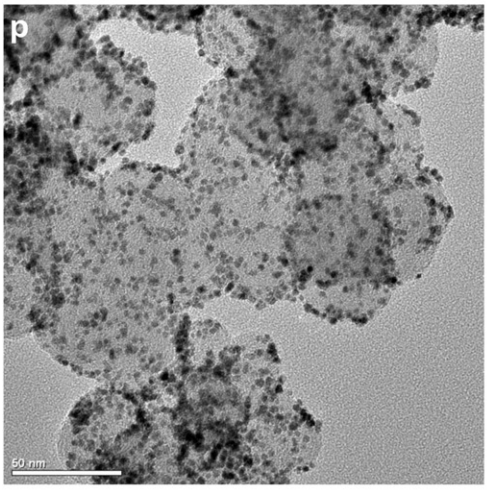


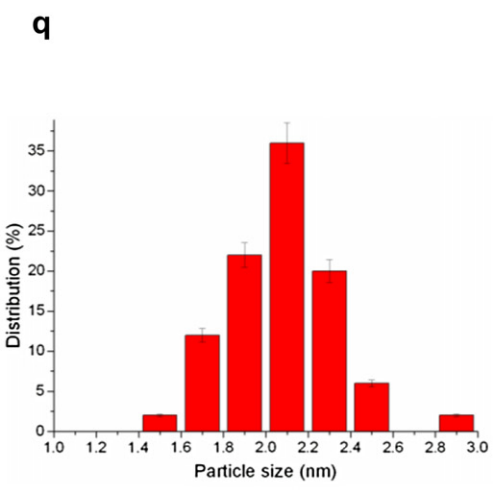


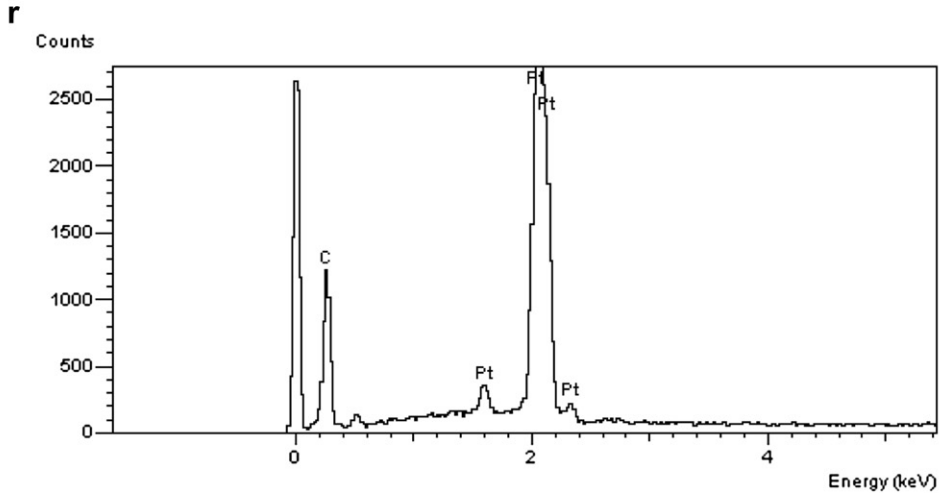


**Fig. 3.** (*continued*).

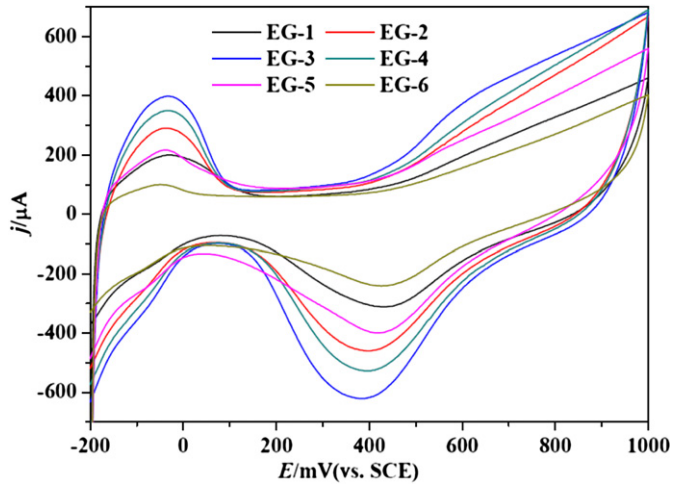


**Fig. 4.** CVs at the electrodes prepared by samples synthesized under different conditions in 0.5 M $HClO_4$ at a scan rate of 50 mV $s^{-1}$.

nucleation and growth of Pt nanoparticles. When the hydrolysis step reached completion, the pH values of the suspensions were recorded for complementary analysis with the particle sizes calculated from XRD.

The XRD patterns of the samples synthesized under different conditions, shown in Fig. 1, were used to determine the Pt particle size and crystallization state of the samples. As observed in the curves, the Pt atoms in every sample exhibit a face-centered cubic (fcc) structure, i.e., the amount of urea added did not affect the crystallization of the Pt nanoparticles. The Pt particle sizes were calculated from full width at half height of the (220) peaks using the Scherrer formula [22]:

$$D = K\lambda/\beta\cos\theta \quad (2)$$

where $K$ is a constant equal to 0.9, $\lambda$ is the X-ray wavelength (1.54056 Å for Cu Kα radiation), $\beta$ is the full width at half height of the diffraction peak (in radians), and $\theta$ is the angle corresponding to the peak maximum.

The pH change after the urea hydrolysis step and the calculated Pt particle size as a function of the amount of urea added were displayed in Fig. 2. As the urea content increased, the pH increased and the particle size decreased. For 100–300 mg of urea, the variation of pH and particle size is slow, implying that the hydrolysis reaction reaches an equilibrium in this concentration range.

Fig. 3 shows TEM micrographs, the corresponding size distribution histograms (including the error bars), and the corresponding EDX results for EG-1–EG-6. The TEM micrographs show that the Pt nanoparticles are highly aggregated on the carbon support in EG-1 and EG-2 and better dispersed in EG-3–EG-6. Furthermore, the histogram indicates that the mean Pt particle sizes are 3.76, 2.72, 2.47, 2.39, 2.28, and 2.10 nm for EG-1, EG-2, EG-3, EG-4, EG-5, and EG-6, respectively, which is consistent with the regular pattern found in the XRD results. The EDX results indicate that the Pt content of EG-1, EG-2, EG-3, EG-4, EG-5, and EG-6 was 59.93, 60.97, 60.10, 60.05, 60.62, and 60.70, respectively, which prove the complete reduction of elemental Pt.

These physical characterizations reveal that the use of EG as a solvent and a weak reducing agent is favorable for Pt dispersion and the controllability of the Pt particle size in the urea buffer.

Fig. 4 shows the cyclic voltammograms (CVs) of the samples recorded in 0.5 M $HClO_4$ at a scan rate of 50 mV $s^{-1}$ at the electrode. Based on the areas of the H adsorption-desorption peaks, the ESA order is EG-3 > EG-4 > EG-2 > EG-5 > EG-1 > EG-6. With increasing particle size, the ESAs of the Pt/C catalysts first increased, peaked at EG-3, and then decreased. Thus, there is an optimal Pt particle size in terms of ESA.

The CVs of DME electrooxidation in 0.5 M $HClO_4$ solution saturated with DME at a scan rate of 25 mV $s^{-1}$ are shown in Fig. 5, in which the forward scan peak current can be used to determine the catalytic activity for DME electrooxidation. The peak potential does not shift significantly among the samples, nor is there a distinct change in the peak shape. The results suggest that the electrooxidation mechanism and surface properties of the catalyst have not been affected by the Pt particle size. The peak current increased with increasing Pt particle size until EG-3, at which point it began to decrease. Thus, there is also an optimal Pt particle size in terms of the use of Pt as an anode catalyst.

Regarding the number of electrons involved in the electrooxidation of DME on the samples, Fig. 6(a)–(f) show the CVs at different scan rates in 0.5 M $HClO_4$ solution. The electrooxidation of DME is an irreversible electron transfer process, and the peak potentials shift positively with increasing scan rates. Fig. 6(g) shows the relationship between the peak current and the square root of the scan rate. The linear relationship suggests that DME electrooxidation is diffusion-controlled. The relationship between the peak current and the square root of scan rates adheres to the following equation:

$$i_p = 2.99 \times 10^5 n(\alpha n')^{1/2} A C_\infty D_0^{1/2} v^{1/2} \quad (3)$$

where $i_p$ is the peak current, $n$ is the number of electrons transferred in the overall reaction, $n'$ is the number of electrons transferred in the rate-determining step, $\alpha$ is the electron transfer coefficient in the rate-determining step, $A$ is the electrode surface area, $C_\infty$ is the bulk concentration of the reactant, $D_0$ is the diffusion coefficient of the reactant, and $v$ is the potential scan rate. The slope of the $i_p$ vs. the square root of scan rate is $2.99 \times 10^5 n(\alpha n')^{1/2} A C_\infty D_0^{1/2}$. In the same electrolyte and for the same reaction, the parameters $n$, $C_\infty$ and $D_0$ are constant; therefore, the slope is determined by $\alpha n'$. The corresponding slopes of samples EG-1, EG-2, EG-3, EG-4, EG-5, and EG-6 are 95.875, 104.833, 129.673, 117.286, 74.013, and 42.242, respectively. The slope first increases and then decreases with increasing Pt particle size, peaking at EG-3, which is consistent with the results from the H adsorption-desorption peak and CV of DME electrooxidation.

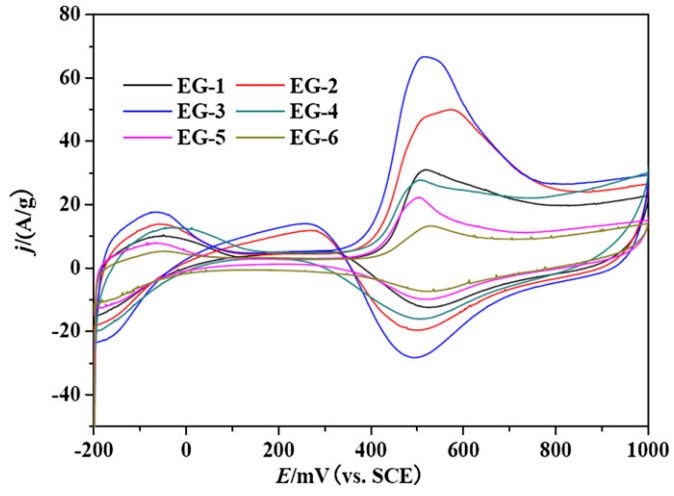


**Fig. 5.** CVs for DME electrooxidation in 0.5 M $HClO_4$ saturated with DME at a scan rate of 25 mV $s^{-1}$ at the electrodes prepared by the samples synthesized under different conditions.

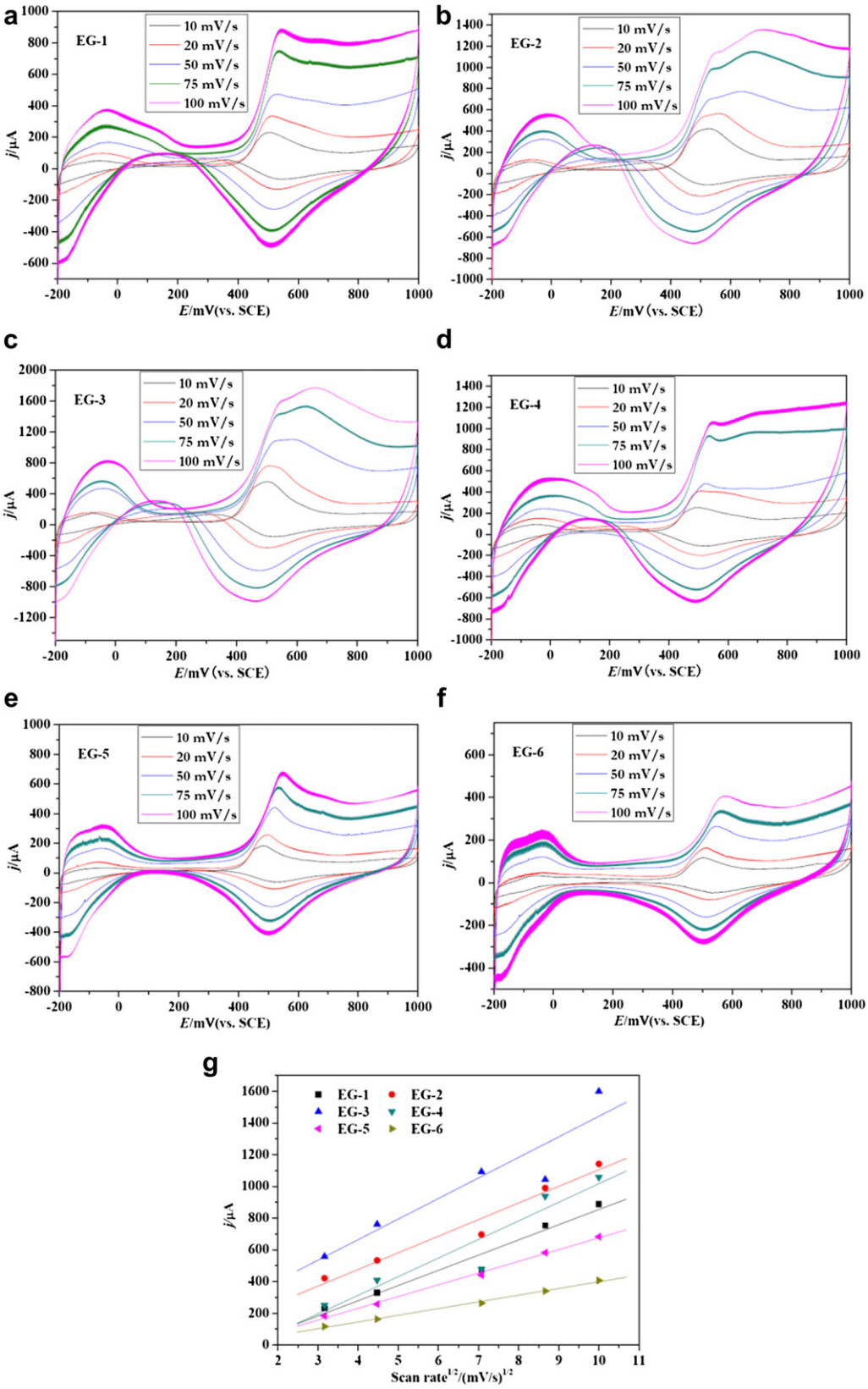


**Fig. 6.** (a)–(f): CVs at electrodes prepared by the samples synthesized under different conditions in 0.5 M $HClO_4$ solution saturated with DME at scan rates of 10, 20, 50, 75, and 100 mV $s^{-1}$. (g): Relationship between peak current and the square root of the scan rate.

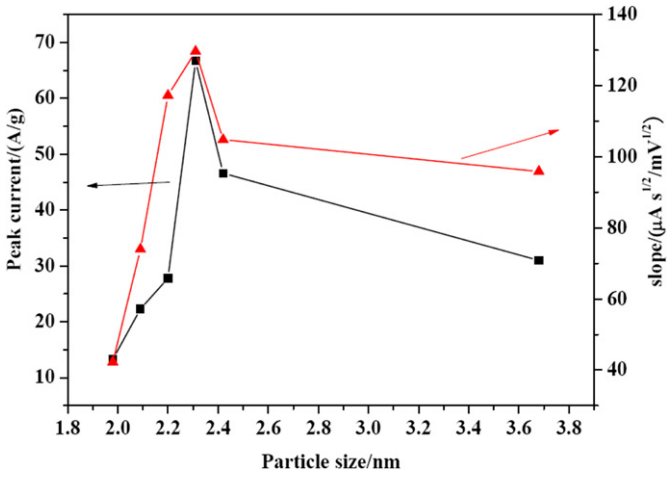


**Fig. 7.** Peak currents for DME electrooxidation from Fig. 5 (left axis) and slopes from Fig. 6(g) (right axis) as functions of Pt nanoparticle sizes (horizontal axis).

The relationships between the DME electrooxidation peak current from Fig. 5 and the Pt nanoparticle size and that between the DME electrooxidation peak current from Fig. 5 and the slopes from Fig. 6(g) are shown in Fig. 7, revealing a distinct parabolic trend. The electrode prepared by EG-3 possesses the highest electrocatalytic activity, corresponding to the highest electron transfer coefficient within the series of catalysts.

## 4. Conclusion

A synthetic method for a Pt nanoparticle catalyst that provides controllable particle size without any surfactant has been successfully developed. The XRD and TEM results indicated that the Pt nanoparticles were well dispersed and that the particle size decreases with increasing urea content. Furthermore, the Pt particle size has a significant effect on the electroactive surface area, electrocatalytic activity for DME electrooxidation and electron transfer coefficient. The CVs of H adsorption-desorption, DME electrooxidation and DME saturated solution at different scan rates show that the electroactive surface area and DME electrooxidation activity of the prepared catalysts as well as the electron transfer coefficient of the electrode reaction all exhibit a parabolic relationship with Pt particle size. The existence of an optimal Pt particle size is similar to that observed for the use of Pt catalysts in methanol or hydrogen electrooxidation [23,24]. Because DME is a promising new fuel cell fuel with an unclear electrooxidation mechanism, these results are important for determining the DME electrooxidation mechanism and designing anode catalysts for DDFCs.

## Acknowledgments

We gratefully thank the reviewers for their valuable suggestions and comments. This work was financially supported by the National Natural Science Foundation of China (20933004, 21011130027, 21073180, 21271168), the High Technology Research Program (863 program, 2007AA05Z159, 2007AA05Z143 and 2009AA05Z111) of the Science and Technology Ministry of China, and the Jilin Province Science and Technology Development Program (20100102).

## References

[1] T.A. Semelsberger, R.L. Borup, H.L. Greene, Journal of Power Sources 156 (2006) 497–511.
[2] A. Serov, C. Kwak, Applied Catalysis B Environmental 91 (2009) 1–10.
[3] G. Kerangueven, C. Coutanceau, E. Sibert, J.M. Leger, C. Lamy, Journal of Power Sources 157 (2006) 318–324.
[4] I. Mizutani, Y. Liu, S. Mitsushima, K.I. Ota, N. Kamiya, Journal of Power Sources 156 (2006) 183–189.
[5] M.M. Mench, H.M. Chance, C.Y. Wang, Journal of the Electrochemical Society 151 (2004) A144–A150.
[6] K.D. Cai, G.P. Yin, J.J. Wang, L.L. Lu, Energy & Fuels 23 (2009) 903–907.
[7] T. Haraguchi, Y. Tsutsumi, H. Takagi, N. Tamegai, S. Yamashita, Electrical Engineering in Japan 150 (2005) 19–25.
[8] G. Kerangueven, C. Coutanceau, E. Sibert, F. Hahn, J.M. Leger, C. Lamy, Journal of Applied Electrochemistry 36 (2006) 441–448.
[9] Y. Liu, S. Mitsushima, K. Ota, N. Kamiya, Electrochimica Acta 51 (2006) 6503–6509.
[10] Y. Tong, L. Lu, Y. Zhang, Y. Gao, G. Yin, M. Osawa, S. Ye, Journal of Physical Chemistry C 111 (2007) 18836–18838.
[11] Q. Zhang, Z.F. Li, S.W. Wang, W. Xing, R.J. Yu, X.J. Yu, Electrochimica Acta 53 (2008) 8298–8304.
[12] L.L. Lu, G.P. Yin, Z.B. Wang, Y.Z. Gao, Electrochemistry Communications 11 (2009) 1596–1598.
[13] F. Si, X. Chen, L. Liang, C. Li, J. Liao, C. Liu, X. Zhang, W. Xing, Electrochimica Acta 56 (2011) 5966–5971.
[14] L.L. Lu, G.P. Yin, Z.B. Wang, K.D. Cai, Y.Z. Gao, Catalysis Communications 10 (2009) 971–974.
[15] L.L. Lu, G.P. Yin, Y.J. Tong, Y. Zhang, Y.Z. Gao, M. Osawa, S. Ye, Journal of Electroanalytical Chemistry 619 (2008) 143–151.
[16] L.L. Lu, G.P. Yin, Y.J. Tong, Y. Zhang, Y.Z. Gao, M. Osawa, S. Ye, Journal of Electroanalytical Chemistry 642 (2010) 82–91.
[17] Y. Zhang, L.L. Lu, Y.J. Tong, M. Osawa, S. Ye, Electrochimica Acta 53 (2008) 6093–6103.
[18] Z. Xu, H. Zhang, H. Zhong, Q. Lu, Y. Wang, D. Su, Applied Catalysis B Environmental 111 (2012) 264–270.
[19] W. Sheng, S. Chen, E. Vescovo, Y. Shao-Horn, Journal of the Electrochemical Society 159 (2012) B96–B103.
[20] S.E.H. Murph, C.J. Murphy, H.R. Colon-Mercado, R.D. Torres, K.J. Heroux, E.B. Fox, L.B. Thompson, R.T. Haasch, Journal of Nanoparticle Research 13 (2011) 6347–6364.
[21] B. Fang, N.K. Chaudhari, M.S. Kim, J.H. Kim, J.S. Yu, Journal of the American Chemical Society 131 (2009) 15330–15338.
[22] B.E. Warren, X-ray Diffraction, Dover Publications, 1969.
[23] T. Frelink, W. Visscher, J.A.R. van Veen, Journal of Electroanalytical Chemistry 382 (1995) 65.
[24] S. Mukerjee, Journal of Applied Electrochemistry 20 (1990) 537.